

University of Nebraska - Lincoln

DigitalCommons@University of Nebraska - Lincoln

Faculty Publications from Nebraska Center for
Materials and Nanoscience

Materials and Nanoscience, Nebraska Center
for (NCMN)

2-8-2017

Cooperative and noncooperative magnetization reversal in alnicos

Raplh Skomski

University of Nebraska - Lincoln, rskomski2@unl.edu

Liqin Ke

Iowa State University

Matthew J. Kramer

Iowa State University

Iver E. Anderson

Iowa State University

C.Z. Wang

Iowa State University

See next page for additional authors

Follow this and additional works at: <https://digitalcommons.unl.edu/cmrafacpub>



Part of the [Atomic, Molecular and Optical Physics Commons](#), [Condensed Matter Physics Commons](#), [Engineering Physics Commons](#), and the [Other Physics Commons](#)

Skomski, Raplh; Ke, Liqin; Kramer, Matthew J.; Anderson, Iver E.; Wang, C.Z.; Zhang, W.Y.; Shield, Jeff E.; and Sellmyer, D. J., "Cooperative and noncooperative magnetization reversal in alnicos" (2017). *Faculty Publications from Nebraska Center for Materials and Nanoscience*. 126.
<https://digitalcommons.unl.edu/cmrafacpub/126>

This Article is brought to you for free and open access by the Materials and Nanoscience, Nebraska Center for (NCMN) at DigitalCommons@University of Nebraska - Lincoln. It has been accepted for inclusion in Faculty Publications from Nebraska Center for Materials and Nanoscience by an authorized administrator of DigitalCommons@University of Nebraska - Lincoln.

Authors

Raph Skomski, Liqin Ke, Matthew J. Kramer, Iver E. Anderson, C.Z. Wang, W.Y. Zhang, Jeff E. Shield, and D. J. Sellmyer

Cooperative and noncooperative magnetization reversal in alnicos

Ralph Skomski,¹ Liqin Ke,² Matthew J. Kramer,² Iver E. Anderson,²
C. Z. Wang,² W. Y. Zhang,¹ Jeff E. Shield,² and D. J. Sellmyer¹

¹Nebraska Center for Materials and Nanoscience and Department of Physics and Astronomy,
University of Nebraska, Lincoln, Nebraska 68588, USA

²Ames Laboratory, Iowa State University, Ames, Iowa 50011, USA

³Department of Mechanical and Materials Engineering, University of Nebraska, Lincoln,
Nebraska 68588, USA

(Presented 2 November 2016; received 25 September 2016; accepted 12 November 2016;
published online 8 February 2017)

It is investigated how magnetostatic interactions affect the coercivity of alnico-type magnets. Starting from exact micromagnetic relations, we analyze two limits, namely cooperative reversal processes operative on short length scales and noncooperative reversal processes on long length scales. In alnicos, intrawire interactions are predominantly cooperative, whereas interwire effects are typically noncooperative. However, the transition between the regimes depends on feature size and hysteresis-loop shape, and interwire cooperative effects are largest for nearly rectangular loops. Our analysis revises the common shape-anisotropy interpretation of alnicos. © 2017 Author(s). All article content, except where otherwise noted, is licensed under a Creative Commons Attribution (CC BY) license (<http://creativecommons.org/licenses/by/4.0/>). [<http://dx.doi.org/10.1063/1.4976216>]

I. INTRODUCTION

In spite of several decades of research, the magnetization reversal in alnico permanent magnets¹⁻⁵ has remained poorly understood. This question is of great practical importance, because the coercivity is the “bottleneck” limiting the use of this otherwise very good permanent-magnet material.^{2-4,6} Alnicos have, essentially, a nanostructure where columnar regions of ferromagnetic Fe₆₅Co₃₅ nanorods or “wires” are dispersed in a nonmagnetic Ni-Al matrix. The magnetic anisotropy of alnico magnets is predominantly of magnetostatic origin. *Magnetocrystalline* anisotropy, K_1 , is very small in alnicos, although there are ongoing efforts to introduce nonnegligible magnetocrystalline anisotropy.⁷⁻⁹

Conventional wisdom is that the coercivity of alnicos is due to shape anisotropy, that is, the behavior of the embedded Fe-Co rich wires in the alnico matrix is very similar to that of small elongated Stoner-Wohlfarth particles.^{10,11} However, this comparison is questionable for two reasons. First, Stoner-Wohlfarth-like coherent rotation is limited to wire diameters of up to about 20 nm,¹²⁻¹⁴ whereas typical alnico wires have thicknesses in excess of 50 nm. In these relatively thick wires, magnetization reversal proceeds through the stage of magnetization curling.^{3,12-15} For ellipsoids of revolution, there exist exact solutions of the curling problem, whereas nonellipsoidal shapes require numerical calculations.^{16,17} Nevertheless, a full solution of the alnico coercivity problem, including interwire interactions, is not possible using contemporary computer technology.

Second, different rods interact with each other, which affects the coercivity. These interactions are often approximated by an effective interaction field that depends on the packing fraction of the rods. The effect of the packing fraction was first mentioned by Kittel in 1949, Eq. 6.2.24 in Ref. 18, although the underlying model, Fig. 49 in the same article, is incompatible with the exact results^{12,15} for ellipsoids of revolution. A similar approach was used in Ref. 19, reproducing the packing-fraction dependence of the energy product.

However, neither the curling mode nor the interactions between the rods are consistent with shape anisotropy, which is defined by

$$K_{\text{sh}} = \frac{1}{2} (1 - 3\mathcal{D}) \mu_0 M_s^2 \quad (1)$$

where \mathcal{D} is the demagnetizing factor of the particles.²⁰ The demagnetizing field $-\mathcal{D}M$ corresponding to \mathcal{D} is related to but should not be confused with the internal magnetic field, which has a much broader meaning²¹ and includes the above effective fields, for example.

The aim of this paper is to show that and explain why the shape-anisotropy picture of Eq. (1) is not applicable to alnico magnets.

II. MEANING OF SHAPE ANISOTROPY

Let us start with the *exact* nucleation-field coercivity for homogeneous ellipsoids of revolution.^{12,14,15} Assuming, for simplicity, that $K_1 = 0$, Eqs. (4.10-11) in Ref. 14 become

$$H_c = \frac{1}{2} (1 - 3\mathcal{D}) M_s \quad (2)$$

and

$$H_c = -\mathcal{D} M_s + \frac{c(\mathcal{D})A}{\mu_0 M_s R^2} \quad (3)$$

Here A is the exchange stiffness, the radius R refers to the two degenerate axes of the ellipsoid, and $c = 8.666$ for spheres ($\mathcal{D} = 1/3$) and $c = 6.678$ for long ellipsoidal rods ($\mathcal{D} = 0$). Equations (2) and (3) describe coherent rotation and curling, respectively, and the physically realized nucleation field is the smaller of the two H_c values.

Evaluation of Eqs. (2-3) shows that coherent rotation dominates for wires with radii smaller than about $R_c = 10$ nm, which can also be shown experimentally.¹³ Alnico rods are essentially described by Eq. (3), which bears no resemblance to the shape anisotropy expression of Eq. (1). In fact, since $\mathcal{D} \approx 0$ and $c \approx 8.666$, the coercivity is almost entirely determined by the rod diameter: $H_c \sim 1/R^2$. Figure 1 summarizes the problem, namely that shape anisotropy is not a well-defined concept for $R > R_c$.

In fact, comparing the limits $R < R_c$, or Eq. (2), and $R = \infty$ in Eq. (3) shows that these two equations correspond to shape anisotropy in small particles (2) and demagnetizing fields ($-\mathcal{D} M_s$) in large particles (3). In particular, the demagnetizing field, $-\mathcal{D} M_s$, is always *negative* and never yields a positive contribution to anisotropy field and coercivity. In the following section, we will see that this feature is deeply rooted in the micromagnetism and not restricted to ellipsoidal shapes.

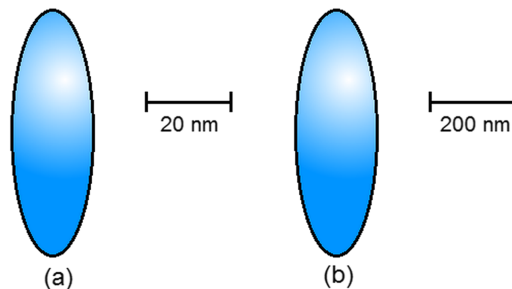


FIG. 1. Shape anisotropy and size scaling. Both magnets are made from the same materials and have the same shape, but the coercivity of (b) is about 100 times smaller than that of (a).

III. ANALYSIS OF MAGNETOSTATIC INTERACTIONS

To describe structurally inhomogeneous magnets, we start from the micromagnetic free energy¹⁴

$$\mathcal{F} = \int \left\{ A \left[\nabla \left(\frac{\mathbf{M}}{M_s} \right) \right]^2 - K_1 \frac{(\mathbf{n} \cdot \mathbf{M})^2}{M_s^2} - \mu_0 \mathbf{M} \cdot \mathbf{H} - \frac{\mu_0}{2} \mathbf{M} \cdot \mathbf{H}_d(\mathbf{M}) \right\} d\mathbf{r} \quad (4a)$$

where $M_s(\mathbf{r}) = J_s(\mathbf{r})/\mu_0$ is the spontaneous magnetization, $K_1(\mathbf{r})$ denotes the first uniaxial anisotropy constant, and the unit vector $\mathbf{n}(\mathbf{r})$ the local anisotropy direction. \mathbf{H} is the external magnetic field, and \mathbf{H}_d is the magnetostatic self-interaction field:

$$\mathbf{H}_d(\mathbf{r}) = \frac{1}{4\pi} \int \frac{3(\mathbf{r} - \mathbf{r}')(\mathbf{r} - \mathbf{r}') \cdot \mathbf{M}(\mathbf{r}') - |\mathbf{r} - \mathbf{r}'|^2 \mathbf{M}(\mathbf{r}')}{|\mathbf{r} - \mathbf{r}'|^5} dV' \quad (4b)$$

The parameters entering Eq. (4) are all local, that is, they depend on local chemistry, crystal structure, and crystallite orientation. The equation is very general and includes, for example, the NiAl-rich matrix phase, where $A = M = K_1 = 0$ in good approximation. Hysteresis loops are obtained by tracing rotations of the local magnetization vector $\mathbf{M}(\mathbf{r})$ as a function of the applied field H .

To elucidate the origin of alnico coercivity, we must analyze the magnetostatic selfinteraction energy $E_{MS} = -1/2 \mu_0 \int \mathbf{M} \cdot \mathbf{H}_d d\mathbf{r}$. This integral can also be written as

$$E_{MS} = 1/2 \int \mathcal{K}(\mathbf{r}, \mathbf{r}') \mathbf{M}(\mathbf{r}) \mathbf{M}(\mathbf{r}') d\mathbf{r} d\mathbf{r}' \quad (5)$$

where $\mathcal{K}(\mathbf{r}, \mathbf{r}')$ is the dipolar interaction kernel implied in Eq. (4b). The key question is the treatment of the product $\mathbf{M}(\mathbf{r}) \mathbf{M}(\mathbf{r}')$. There are two limiting cases, which are outlined in Figure 2 and correspond to shape anisotropy (a) and to an interaction with local demagnetizing fields (b).

When \mathbf{r} and \mathbf{r}' are close together, as in Fig. 2(a), the interatomic exchange ensures that $\mathbf{M}(\mathbf{r}) \approx \mathbf{M}(\mathbf{r}')$ and Eq. (5) becomes

$$E_{MS} = \sum_{ij} \int K_{ij}(\mathbf{r}) M_i(\mathbf{r}) M_j(\mathbf{r}) d\mathbf{r} \quad (6)$$

In this equation, $K_{ij}(\mathbf{r}) = 2 \int \mathcal{K}(\mathbf{r}, \mathbf{r}') d\mathbf{r}'$ has the character of a *shape-anisotropy tensor* and $M_i = (M_x, M_y, M_z)$ is the local magnetization vector. For ellipsoids of revolution, this expression reproduces Eq. (1). For arbitrary geometries, $K_{ij}(\mathbf{r})$ remains a local quantity, but the 9 matrix elements of the tensor K_{ij} are not independent, and by principal-axis transformation, they can be mapped onto the two independent lowest-order anisotropy constants K_1 and K_1' .²²

In the opposite limit of well-separated regions, Fig. 2(b), it is useful to exploit the identity

$$\mathbf{M}(\mathbf{r}) \mathbf{M}(\mathbf{r}') = \mathbf{M}_{av} \mathbf{M}(\mathbf{r}) + \mathbf{M}_{av} \mathbf{M}(\mathbf{r}') + \mathbf{M}_{av}^2 + C(\mathbf{r}, \mathbf{r}') \quad (7)$$

where $\mathbf{M}_{av} = \mathbf{M}_{av}(H)$ is the magnet's average magnetization and

$$C(\mathbf{r}, \mathbf{r}') = (\mathbf{M}(\mathbf{r}) - \mathbf{M}_{av})(\mathbf{M}(\mathbf{r}') - \mathbf{M}_{av}) \quad (8)$$

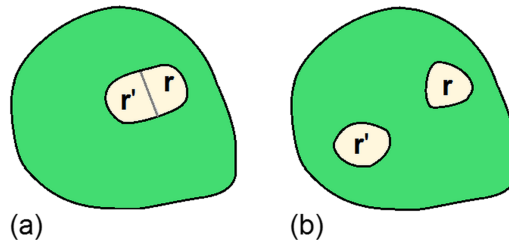


FIG. 2. Geometrical aspects of micromagnetic interactions in magnets: (a) cooperative and (b) noncooperative.

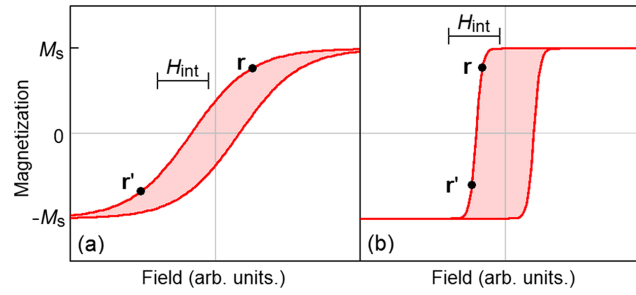


FIG. 3. Cooperative phenomena on the hysteresis loop: (a) noncooperative and (b) cooperative. Cooperativity means the interaction field H_{int} between two magnetic regions at \mathbf{r} and \mathbf{r}' is larger than the difference in the switching fields of the regions.

is the magnetization correlation function. Assuming that the magnetization at \mathbf{r} and \mathbf{r}' are uncorrelated ($C = 0$) and substituting Eq. (7) into Eq. (5) yields

$$E_{\text{MS}} = \mu_0 \int \mathbf{H}_{\text{eff}}(\mathbf{r}) \mathbf{M}(\mathbf{r}) d\mathbf{r} \quad (9)$$

where $\mathbf{H}_{\text{eff}}(\mathbf{r}) = \int \mathcal{K}(\mathbf{r}, \mathbf{r}') \mathbf{M}_{\text{av}} d\mathbf{r}'$ is an effective field. In other words, noncooperative magnetostatic interactions can be mapped onto a local interaction or “demagnetizing” field.

The present analysis shows that the shape anisotropy operates on very small length scales, whereas macroscopic interactions are better understood in terms of effective interaction or demagnetizing fields, in close analogy to Eqs. (2–3). However, the transition between these two limits is nontrivial. Intrawire interactions in alnicos are essentially of the curling type and cannot be mapped onto shape anisotropy, but this does not mean that intrawire cooperative effects are unimportant. The appearance of the exchange stiffness A in Eq. (3) indicates some degree of cooperativity. Physically, magnetostatic interactions yield a flux-closure contribution to the magnetization, but the interatomic exchange prevents this curling from completely destroying coercivity.

Somewhat different considerations apply to the “interwire interactions” between rods. These interactions also exist for curling, because $M_z(\mathbf{r}) \approx M_s$ at the onset of curling, irrespective of the chirality of the individual wire modes. Based on length-scale considerations, one may expect that individual wires reverse noncooperatively. This consideration is basically correct, but there is a caveat. Interwire interactions generally correspond to small interaction fields H_{int} , but when the hysteresis loops are nearly square, as expected for good permanent magnets, the small H_{int} may nevertheless qualitatively interfere with the magnetization reversal. Figure 3 visualizes this mechanism: Different regions \mathbf{r} and \mathbf{r}' of a magnet reverse at different switching fields, but if these switching fields are close together, then H_{int} can strongly affect the reversal. For example, magnetostatic interactions between wires may yield “macroscopic” curling modes that involve several wires but look otherwise similar to intrawire curling modes.

IV. DISCUSSION AND CONCLUSIONS

The mechanisms discussed in this paper have a number of interesting implications. Figure 3 indicates that the micromagnetic susceptibility $\chi = dM/dH$ is important for the understanding of cooperative effects. Similar susceptibility effects are encountered in other areas of physics. For example, the Stoner transition from paramagnetism to ferromagnetism can be described by $\chi = \chi_0 / (1 - \beta \chi_0)$, where χ_0 is the interaction-free Pauli susceptibility and β is proportional to the Stoner exchange.²²

Interaction effects are most pronounced for nearly rectangular loops, that is for the magnets of primary interest in permanent magnetism. At the same time, this limit is the most difficult one to treat by numerical calculation, and efforts¹⁷ are being made to move towards a better numerical understanding of alnico magnets. This includes both intrawire effects, such as coercivity-enhancing features at wire ends, and interwire interactions.

An interesting feature of alnicos, closely related to the topic of the paper, is the analysis of alnico coercivity in terms of the Kronmüller equation

$$H_c = \alpha 2K_1/\mu_0 M_s - \mathcal{D}_{\text{eff}} M_s \quad (10)$$

where α is a dimensionless factor. The effective demagnetizing factor \mathcal{D}_{eff} is an effective *local* demagnetizing factor constant, only loosely related to the macroscopic demagnetizing factor \mathcal{D} .²³ It is often of the order of 1/3, but a notable exception is alnico, where \mathcal{D}_{eff} is actually *negative* on account of the columnar microstructure magnets.

In summary, our analysis shows that the term “shape anisotropy” is misleading when used to explain the anisotropy of alnico magnets. In a strict sense, shape anisotropy is limited to particles or wires having very small diameters. In the opposite limit of macroscopic magnetism, the magnetostatic interactions have the character of demagnetizing fields. The behavior of alnico magnets is complex, closer to the macroscopic limit than to the shape-anisotropy limit, but involves residual cooperative effects crucial for the understanding of alnico coercivity. Future calculations, especially numerical simulations, are necessary to quantitatively understand magnetization reversal in the materials and to exploit the presently discussed mechanisms to improve the coercivity of alnico magnets.

ACKNOWLEDGMENTS

This research is supported by the USDOE-EERE-VTO-EDT program under the DREaM project at Ames Laboratory through contract no. DE-AC02-07CH11358 for a portion of the work and by NCMN for the remainder of the tasks.

- ¹ T. Mishima, “Nickel-aluminum steel for permanent magnets,” *Ohm* **19**, 353 (1932).
- ² R. M. Bozorth, *Ferromagnetism* (van Nostrand, Princeton, New Jersey, 1951).
- ³ R. A. McCurrie, *Ferromagnetic Materials—Structure and Properties* (Academic Press, London, 1994).
- ⁴ L. Zhou, M. K. Miller, P. Lu, L. Ke, R. Skomski, H. Dillon, Q. Xing, A. Palasyuk, M. R. McCartney, D. J. Smith, S. Constantinides, R. W. McCallum, I. E. Anderson, V. Antropov, and M. J. Kramer, “Architecture and magnetism of alnico,” *Acta Materialia* **74**, 224–233 (2014).
- ⁵ R. Skomski, E. Schubert, A. Enders, and D. J. Sellmyer, “Kondorski reversal in magnetic nanowires,” *J. Appl. Phys.* **115**, 17D137-1-3 (2014).
- ⁶ R. Skomski and J. M. D. Coey, *Permanent Magnetism* (Institute of Physics, Bristol, 1999).
- ⁷ R. Skomski, P. Manchanda, P. Kumar, B. Balamurugan, A. Kashyap, and D. J. Sellmyer, “Predicting the future of permanent-magnet materials” (invited), *IEEE Trans. Magn.* **49**(7), 3215–3220 (2013).
- ⁸ R. W. McCallum, L. H. Lewis, R. Skomski, M. J. Kramer, and I. E. Anderson, “Practical aspects of modern and future permanent magnets,” *Ann. Rev. Mater. Res.* **44**, 451–477 (2014).
- ⁹ W. Y. Zhang, R. Skomski, A. Kashyap, S. Valloppilly, X. Z. Li, J. E. Shield, and D. J. Sellmyer, “Coercivity and nanostructure of melt-spun Ti-Fe-Co-B-based alloys,” *AIP Adv.* **6**(5), 056001 (2016).
- ¹⁰ F. E. Luborsky, L. I. Mendelsohn, and T. O. Paine, “Reproducing the properties of alnico permanent magnet alloys with elongated single domain cobalt iron particles,” *J. Appl. Phys.* **28**, 344–351 (1957).
- ¹¹ S. Chikazumi, *Physics of Magnetism* (Wiley, New York, 1964).
- ¹² W. F. Brown, “Virtues and weaknesses of the domain concept,” *Phys. Rev.* **17**, 15–19 (1945).
- ¹³ H. Zeng, R. Skomski, L. Menon, Y. Liu, S. Bandyopadhyay, and D. J. Sellmyer, *Phys. Rev. B* **65**(13), 134426 (2002).
- ¹⁴ R. Skomski, *J. Phys.: Condens. Matter* **15**, R841–896 (2003).
- ¹⁵ A. Aharoni, *Introduction to the Theory of Ferromagnetism* (University Press, Oxford, 1996).
- ¹⁶ J. Fischbacher, S. Bance, M. Gusenbauer, A. Kovacs, H. Oezelt, F. Reichel, and T. Schrefl, “Micromagnetics for the coercivity of nanocomposite permanent magnets,” in *Proc. REPM* (Annapolis, Maryland, 2014), pp. 241–243.
- ¹⁷ L.-Q. Ke *et al.*, in preparation (2016).
- ¹⁸ C. Kittel, “Physical theory of ferromagnetic domains,” *Rev. Mod. Phys.* **21**, 541–583 (1949).
- ¹⁹ R. Skomski, Y. Liu, J. E. Shield, G. C. Hadjipanayis, and D. J. Sellmyer, “Permanent magnetism of dense-packed nanostructures,” *J. Appl. Phys.* **107**, 09A739-1-3 (2010).
- ²⁰ J. A. Osborn, “Demagnetizing factors of the general ellipsoid,” *Phys. Rev.* **67**, 351–357 (1945).
- ²¹ R. Skomski, G. C. Hadjipanayis, and D. J. Sellmyer, “Effective demagnetizing factors of complicated particle mixtures,” *IEEE Trans. Magn.* **43**(6), 2956–2958 (2007).
- ²² R. Skomski, *Simple Models of Magnetism* (University Press, Oxford, 2008).
- ²³ R. Skomski and J. M. D. Coey, “Magnetic anisotropy — How much is enough for a permanent magnet?,” *Scripta Mater.* **112**, 3–8 (2016).